Pergamon

Int. J. Heat Mass Transfer. Vol. 41, Nos 6–7, pp. 851–857, 1998

Printed in Great Britain
0017–9310/98 $19.00+0.00

PII: S0017-9310(97)00180-4

An experimental investigation of single-phase forced convection in microchannels

T. M. ADAMS, S. I. ABDEL-KHALIK,† S. M. JETER and Z. H. QURESHI‡

George Woodruff School of Mechanical Engineering, Georgia Institute of Technology, Atlanta, Georgia 30332-0405, U.S.A.

(*Received* 30 *December* 1996 *and in final form* 7 *June* 1997)

Abstract—Turbulent, single-phase forced convection of water in circular microchannels with diameters of 0.76 and 1.09 mm has been investigated. The data show that the Nusselt numbers for the microchannels are higher than those predicted by traditional large channel correlations. Based on the data obtained in this investigation, along with earlier data for smaller diameter channels, a generalized correlation for the Nusselt number for turbulent, single-phase, forced convection in circular microchannels has been developed. The diameter, Reynolds number, and Prandtl number ranges are 0.102–1.09 mm, 2.6×10^3–2.3×10^4, and 1.53–6.43, respectively. With a confidence level of greater than 95%, differences between experimental and predicted Nusselt number values are less than $\pm 18.6\%$. © 1997 Elsevier Science Ltd.

INTRODUCTION

Highly subcooled single-phase forced convection in microchannels is an effective cooling mechanism with a wide range of applications. Among these are the cooling of such diverse systems as accelerator targets, high power resistive magnets, compact fission reactor cores, fusion reactor blankets, advanced space thermal management systems, manufacturing and materials processing operations, and high-density multi-chip modules in supercomputers and other modular electronics. The power densities in some of these systems (e.g. accelerator targets and high power resistive magnets) reach as high as 4.5 MW l^{-1}. Such power densities are nearly two orders of magnitude higher than the average power density in the core of a current commercial light water reactor.

Since the hydraulic diameter of a microchannel may be comparable to or smaller than the largest eddies in turbulent flow, it has been postulated that the turbulent mechanism for heat and momentum transfer may be suppressed at otherwise turbulent Reynolds numbers [1]. A wide range of empirical Nusselt-type correlations for channel flow have been reported; these were generally obtained using hydraulic diameters of two centimeters or more. The extent to which predictions of these correlations differ from the actual Nusselt numbers for channel diameter $\leqslant 2$ mm has not been well established.

A small number of investigators have looked at turbulent convection in small passages, starting with a study by Levy *et al.* [2] of turbulent forced convection in rectangular channels. The channels measured 2.54×63.5 mm (0.1×2.5 in), the corresponding hydraulic diameter is 4.88 mm. Over the range of Reynolds numbers investigated (10^4–10^5), the data were nearly 30–50% below values of the heat transfer coefficient predicted by the Seider–Tate equation. Of further interest was a study by Lancet [3] of turbulent air flow through gaps measuring 0.58–0.64 mm (0.023–0.025 in). Lancet's data showed a strong dependence of friction factor on surface roughness; at a Reynolds number of 4×10^4, a nearly hydraulically smooth surface produced friction factors nearly twice the values expected for a smooth duct.

Gambill and Bundy [4] studied both momentum and heat transfer in thin rectangular channels with gap sizes ranging from 1.09 to 1.45 mm (0.043–0.057 in) corresponding to hydraulic diameters of 1.91–2.67 mm (0.075–0.105 in). For Reynolds number ranging from 9×10^3 to 2.7×10^5, they found the friction factors to be in relatively good agreement with the Moody diagram, while the heat transfer coefficients were slightly higher than those predicted by the Seider–Tate equation, thus calling into question the earlier results of Levy and Lancet.

Acosta *et al.* [5] studied momentum and mass transport in narrow rectangular channels with hydraulic diameters of 0.96 and 0.38 mm; both laminar and turbulent conditions were studied. Correlations for much larger channels were found to be adequate, and it was reasoned by the heat and mass transfer analogy that the heat transfer correlations should also be valid. It was noted, however, that optically smooth walls were necessary to satisfy the condition of hydraulic smoothness and that both the friction factor and mass transfer coefficient were highly dependent on surface roughness.

In an experimental investigation to verify a theor-

† Author to whom correspondence should be addressed.

‡ Westinghouse Savannah River Company, Aiken, South Carolina.

NOMENCLATURE

A	heat transfer area of microchannel [m^2]	Nu	Nusselt number ($h \cdot D/k_{fl}$)
C	constant in heat transfer enhancement function	Pr	Prandtl number ($\mu \cdot c/k$)
c	specific heat [$kJ\ kg^{-1} \cdot {}^\circ C^{-1}$]	$\dot{Q}$	heat transfer rate [W]
D	inside diameter of microchannel [mm]	Re	Reynolds number ($\rho_{fl} \cdot V \cdot D/\mu_{fl}$)
D_0	reference diameter in equation (9)	V	velocity of water [$m\ s^{-1}$].
f	friction factor		
F	heat transfer enhancement function [equation (9)]	Greek symbols	
$\bar{h}$	average heat transfer coefficient for microchannel	μ	dynamic viscosity [$kg\ (m \cdot s)^{-1}$]
i	enthalpy [$J\ kg^{-1}$]	ρ	density [$kg\ m^{-3}$]
K	parameter in Petukhov correlation	Φ	enhancement ratio (Nu_{exp}/Nu_{pred}).
k	thermal conductivity [$W\ (m \cdot {}^\circ C)^{-1}$]	Subscripts	
LMTD	log mean temperature difference [°C]	fl	fluid
$\dot{m}$	mass flow rate of water [$kg\ s^{-1}$]	Gn	based on the Gnielinski correlation
		in	at fluid inlet
		out	at fluid exit.

etical model for a microelectronic heat sink, Nayak *et al.* [6] employed rectangular flow channels with 1000 μm gaps corresponding to hydraulic diameters of 1.7 mm. The theoretical model was developed by Hwang *et al.* [7] and incorporated standard correlations for both the friction factor and heat transfer coefficient. Nayak found lower temperatures and much higher pressures than predicted by the model. The lower temperature rises could be partially explained by the model's assumption of negligible conduction effects, however, the reason for the large discrepancy in pressure drops was not clear.

Other microelectronic heat sink studies have utilized turbulent convection in small rectangular channels; both theoretical models and experimental investigations have been reported. The experimental works are usually aimed at verifying the theoretical models. For manufacturing ease, however, most of these experiments used large scale test sections rather than actual scale models. (Nayak *et al.* is a notable exception.) Furthermore, the standard heat transfer correlations used in the models were often cited as one of the main sources of error between experiment and theory. In an excellent review of this work, Phillips [8] calls for improved turbulent heat transfer correlations for microchannels, especially for lower Reynolds numbers.

Wang and Peng [9] investigated single-phase forced convection of water and methanol in rectangular microchannels with hydraulic diameters ranging from 0.311 to 0.747 mm. They found that the transition to turbulent flow was initiated at Reynolds numbers of 1000–1500. They also reported that their heat transfer data could be well predicted by a modification of the Dittus–Boelter equation in which the constant has been changed from 0.023 to 0.00805. Liquid temperature, velocity and microchannel size all strongly affected the heat transfer behavior.

Peng and Peterson [10] studied the effect of geometry on single-phase forced convective heat transfer of water in rectangular microchannel grooves on flat plates. The hydraulic diameters of the microchannels varied from 0.311 to 0.367 mm. The frictional pressure drop was generally smaller than would be predicted by traditional friction factor relationships. The Reynolds number for transition to turbulent flow was also smaller than for ordinary channels, in agreement with Wang and Peng [9].

Recognizing the apparent lack of systematic research on heat and momentum transport in microchannels, Yu *et al.* [11] recently studied the fluid flow and heat transfer characteristics of dry nitrogen gas and water in circular tubes of diameters of 19, 52 and 102 micrometers. Both the laminar and turbulent regimes were studied with Reynolds numbers ranging from 250 to nearly 2×10^4 and Prandtl numbers of 0.7–5.0. Friction factors were slightly lower than the Moody chart values for both the laminar and turbulent regimes. Nusselt numbers for the cooling of water in the turbulent regime, however, were considerably higher than would be predicted for larger tubes, suggesting that the Reynolds analogy does not hold for microchannel flow. The heat transfer experiments were performed with water only.

In the above cited literature, there is considerable disagreement as to the effect of small channel size on turbulent convection. Most of the studies involved rectangular channels and did not isolate the possible additional effect of aspect ratio. Furthermore, though gap sizes in these studies were often small fractions of a millimeter, the widths of the flow passages were often much larger. In some cases, the hydraulic diameters

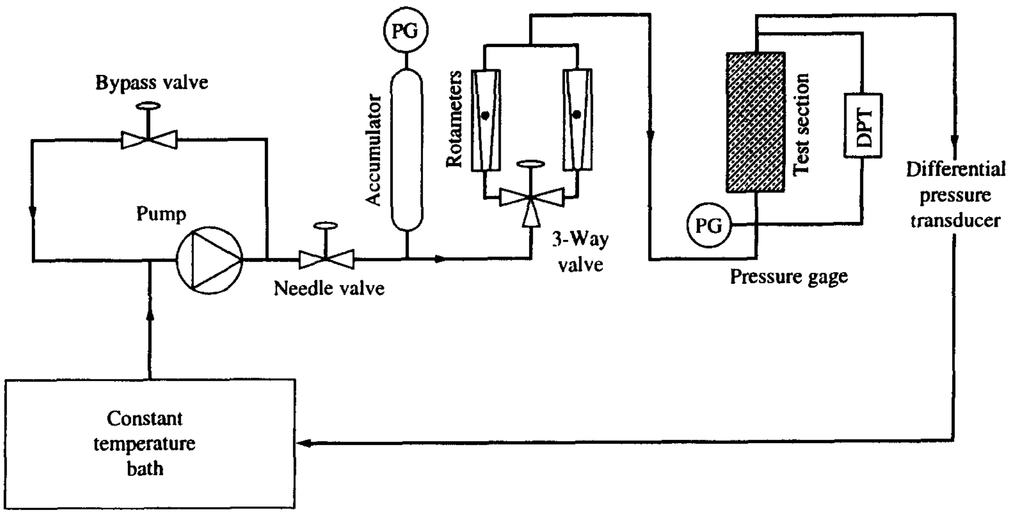

Fig. 1. Schematic of the experimental test loop.

approached or surpassed the 2 mm value for which Kakac *et al.* [1] expressed reservations as to the applicability of traditional correlations. With the exception of Yu *et al.* [11], there seems to be a lack of reliable data on turbulent single phase convection in circular microchannels. More importantly, no reliable experimental evidence has been found as to the smallest size channel for which traditional Nusselt number correlations can be applied without significant error. To this end, this investigation has been undertaken. Single-phase forced convection in circular microchannels with diameters of 0.76 and 1.09 mm has been examined. The channel size range has been selected to complement the data provided by Yu *et al.* [11].

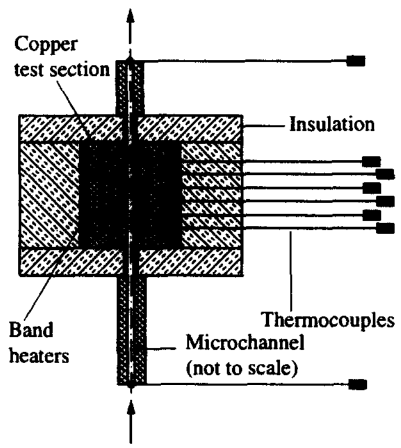

Fig. 2. Details of the 0.76 mm test section.

EXPERIMENTAL APPARATUS AND PROCEDURE

Figure 1 shows a schematic diagram of the experimental test loop. Distilled water in a constant temperature bath at atmospheric pressure is pumped through the test section by a carbon vane pump. A bypass valve provides coarse control of the flow rate, while a needle valve downstream of the pump provides for fine flow rate adjustment. Depending on the flow rate, water enters one of two rotameters before entering the test section itself. Water from the exit of the test section is returned to the constant temperature bath. A bourdon pressure gage measures pressure at the test section inlet. A differential pressure transducer (Rosemount model 1151DP5E22) measures the pressure drop across the test section.

Figure 2 gives a detailed view of the 0.76 mm inner diameter test section. The entire test section is machined from a single piece of solid cylindrical copper. The flow passage was produced using the electrode discharge machining (EDM) technique. An unheated length of 63.5 mm precedes the heated length of 50.8 mm, which is followed by an exit length of 38.1 mm. The entry length is sufficiently long to assure fully developed conditions at the heated section inlet. Both the entry length and the exit length have an outer diameter of 9.53 mm (3/8 in.) to facilitate the use of standard compression fittings. The heated length itself has an outer diameter of 38.1 mm (1 1/2 in.) in order to accommodate the electrical resistance band heaters which surround it, and also to enhance axial conduction so that the boundary condition at the inner diameter more closely approximates a constant temperature rather than a constant heat flux condition. In order to minimize axial heat losses from the heated section, the outer diameter is reduced to 3.2 mm for a length of 12.7 mm on either side of the heated length. Insulation surrounds the entire test section.

Six copper–constantan (type T) thermocouples are embedded in the copper test section at 6.35 mm axial intervals starting at 9.53 mm from the leading edge of the heated section. The radial locations of the thermocouple beads alternate between 12.7 and 6.35 mm. Type T thermocouples are also located at the inlet and the exit of the test section to measure the inlet and exit fluid temperatures. All thermocouples are connected to an EXP-16 multiplexer board which is in turn connected to a DAS-8 data acquisition board installed in a personal computer. Both boards are manufactured by Keithly–Metrabyte.

The 1.09 mm test section is designed in a similar fashion. A schematic diagram of that test section, along with its dimensions, is shown in Fig. 3. Voltage to the band heaters was controlled by use of a Variac transformer, allowing for variable power input. The power was measured by simultaneously measuring the voltage and current to the heaters with multimeters which were calibrated against a calibrated wattmeter. When steady state conditions are reached, typically within 30–60 min, the heat removal rate by the fluid can be measured by applying a macroscopic energy balance:

$$\dot{Q}_{fl} = \dot{m}(i_{out} - i_{in}) \tag{1}$$

where the inlet and exit enthalpies are evaluated at the temperature and pressure of the inlet and exit, respectively. The difference between the calculated heat removal rate by the water and the measured power input was generally less than 10%. Ambient convective losses were estimated and found to be negligible, generally considerably less than 1% of the power input.

The temperatures obtained from the thermocouples in the heated section were used in conjunction with a finite difference model developed with the software EES (Engineering Equation Solver) [12] to obtain the temperature distributions within the copper. The resolution of the calibrated type T thermocouples was ± 0.3°C. Only one thermocouple measurement within the copper was used at a time in the finite difference code. In this way, several temperature distributions were obtained, each based on one measured copper temperature and its location. The differences between

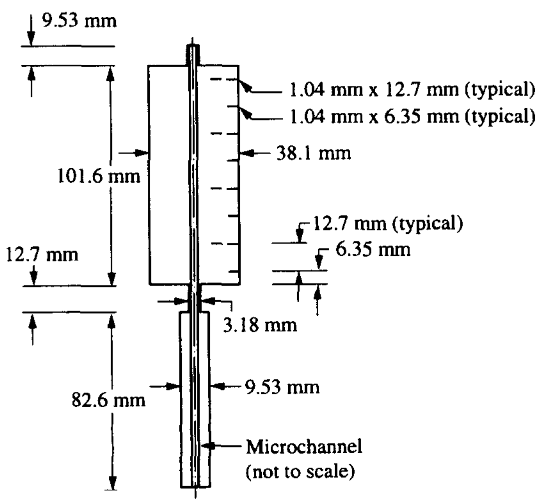

Fig. 3. Dimensions of the 1.09 mm test section.

Table 1. Range of experimental parameters

Diameter	0.76 and 1.09 mm
Velocity	up to 18.9 m s^{-1}
Reynolds number	3.2×10^3–2.3×10^4
Prandtl number	3.7–6.43
Heat flux	up to 3.0 MW m^{-2}

these temperature distributions are primarily due to uncertainties in the individual thermocouple output and its location. The averages of the wall temperatures at the inlet and exit of the heated section were obtained from these finite difference solutions, and then used to define an average log mean temperature difference (LMTD) for the microchannel. This temperature difference, in turn, was used to obtain the average heat transfer coefficient

$$\bar{h} = \frac{\dot{Q}_{fl}}{A \times \mathrm{LMTD}} \tag{2}$$

where A is the area of the inner surface of the heated section. The corresponding Nusselt number was then calculated:

$$Nu = \frac{\bar{h}D}{k_{fl}}. \tag{3}$$

The thermal conductivity of the water was calculated at the average fluid bulk temperature. Table 1 summarizes the overall range of experimental parameters.

RESULTS AND DISCUSSION

It was desired to compare the experimentally obtained Nusselt number data with the best available correlation for the given range of Reynolds and Prandtl numbers. One of the most accurate correlations for single-phase forced convection is that suggested by Petukhov [13]; the correlation has a reported accuracy of $\sim 5\%$:

$$Nu = \frac{(f/8)RePr}{K + 12.7(f/8)^{1/2}(Pr^{2/3} - 1)} \tag{4}$$

where

$$K = 1.07 + (900/Re) - [0.63/(1 + 10Pr)] \tag{5}$$

and f is the D'Arcy friction factor. The correlation is valid for Reynolds numbers and Prandtl numbers in the ranges of 10^4–10^6 and 0.5–2000, respectively. Gnielinski [14] modified the Petukhov correlation to extend the Reynolds number range down to 2300. The Gnielinski correlation is given by

$$Nu = \frac{(f/8)(Re - 1000)Pr}{1 + 12.7(f/8)^{1/2}(Pr^{2/3} - 1)}. \tag{6}$$

The friction factor in equation (6) is calculated using the Filonenko [15] correlation:

$$f = (1.82\log(Re) - 1.64)^{-2}. \tag{7}$$

A significant fraction of our data falls below the lower Reynolds number limit for the Petukhov correlation. Hence, the Gnielinski correlation [equations (6) and (7)] has been used for comparison with the data. Figure 4 shows the variation of the experimental Nusselt numbers with Reynolds number for the two channels examined. Also plotted are curves corresponding to the values of Nusselt number as predicted by the Gnielinski correlation for both the lowest and highest Prandtl numbers covered by the data, namely, 4.21 and 6.43. Clearly, the experimental Nusselt numbers are generally higher than those predicted by the Gnielinski correlation. The deviation between the experimental and predicted Nusselt numbers is more significant for the 0.76 mm microchannel than the 1.09 mm channel. For microchannels, it is clear that a reduction in channel diameter results in further deviation from the predicted Nusselt numbers by traditional large-channel correlations.

Nusselt numbers were also calculated using the largest and smallest LMTD obtained from the finite difference solutions of the temperature distribution. On average, these values varied by only $\pm 3.3\%$ from the value calculated from the average LMTD. These differences are caused by the errors in the individual thermocouple readings used in the finite difference analysis. A detailed analysis using error propagation techniques for all the experimentally measured variables was also performed. Given that the errors in thermocouple readings, mass flow rate, and pressure drop were 0.3°C, 1×10^{-4} kg s^{-1} and 3.4 kPa (0.5 psi), respectively, an average uncertainty estimate of $\pm 13\%$ was calculated. Within this error, the data still consistently fall above the Gnielinski correlation.

It was also desired to compare the Nusselt number data with the data collected by Yu *et al.* for their 0.102 mm diameter channel. Experimental Nusselt numbers were compared to the values predicted by the Gnielinski correlation for the same Reynolds and Prandtl

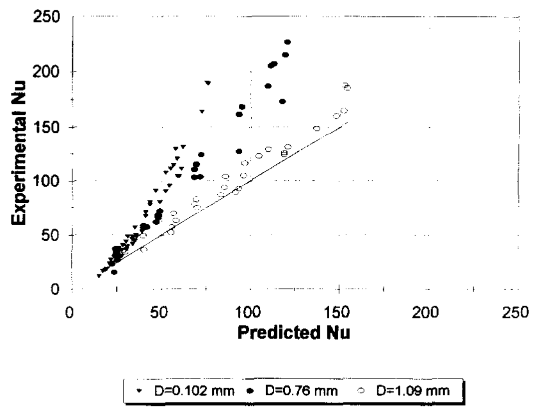

Fig. 5. Comparison of experimental to predicted Nusselt numbers based on the Gnielinski correlation. The data for $D = 0.102$ mm were provided by Yu *et al.* [11].

numbers (Fig. 5). The data are clearly well above the Gnielinski correlation values; for Reynolds numbers near the upper limit of the experimental range, the measured Nusselt numbers for the 0.102 mm diameter channel are nearly two and a half times the predicted value. This enhancement, i.e. the ratio between the experimental Nusselt numbers and those predicted by conventional correlations such as that of Gnielinski, is inversely proportional to microchannel diameter. The data of Yu *et al.* [11] ($D = 0.102$ mm) show the most enhancement, while the 1.09 mm channel examined here shows the least enhancement.

Figure 6 shows the dependence of the enhancement ratio, Φ, defined as the experimental Nusselt number divided by Nusselt number predicted by the Gnielinski correlation, on the microchannel diameter and Reynolds number. For the smallest diameter of 0.102 mm, the enhancement ratio clearly increases with increasing Reynolds number and reaches a value of nearly 2.5 at a Reynolds number of $\sim 2 \times 10^4$. The enhancement ratio for the 0.76 mm microchannel shows a less steep dependence on Reynolds number with a value of ~ 1.8

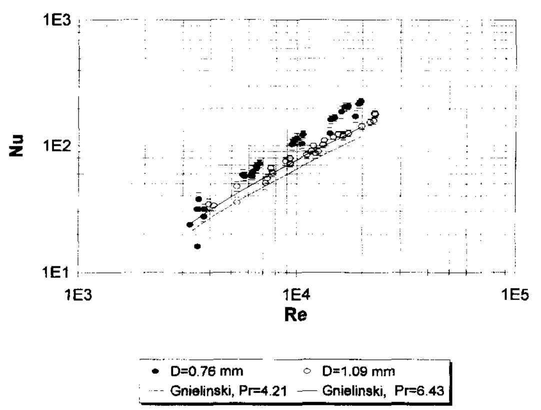

Fig. 4. Comparison of experimental Nusselt numbers to the Gnielinski correlation.

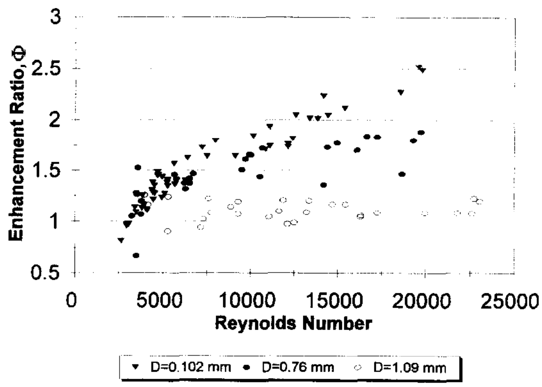

Fig. 6. Reynolds number dependence of the enhancement ratio. The data for $D = 0.102$ mm were provided by Yu *et al.* [11].

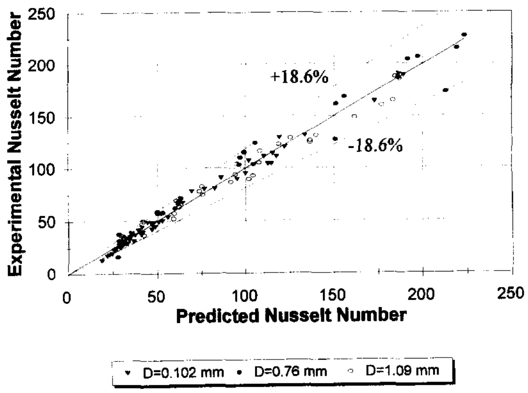

Fig. 7. Comparison of experimental to predicted Nusselt numbers based on equations (8) and (9). The data for $D = 0.102$ mm were provided by Yu *et al.* [11].

at a Reynolds number of nearly 2×10^4. For the largest diameter of 1.09 mm, the enhancement ratio is slightly above unity with no clear dependence on Reynolds number within the examined range.

Given these trends of heat transfer enhancement with diameter and Reynolds number, a modification of the Gnielinski correlation to accommodate the small diameters encountered in microchannels was sought in the following form:

$$Nu = Nu_{Gn}(1+F) \tag{8}$$

where F is given by

$$F = CRe\left(1-\left(\frac{D}{D_0}\right)^2\right). \tag{9}$$

A least-squares fit of all three sets of data gives $C = 7.6 \times 10^{-5}$ and $D_0 = 1.164$ mm. With the correlation cast in this form, D_0 represents the diameter for which equations (8) and (9) predict no enhancement of the Nusselt number over that predicted by the Gnielinski correlation. The diminished heat transfer 'enhancement' as D_0 is approached is evidenced by the data for the 1.09 mm diameter channel. On the other hand, as the diameter becomes vanishingly small, the enhancement ratio predicted by equations (8) and (9) becomes a function of Re only.

Figure 7 gives a comparison of experimental Nusselt numbers to values of Nusselt number predicted by equations (8) and (9). A statistical analysis of the errors between experimental and predicted values reveals that for a 95% confidence level, the differences between the data and predicted values using equations (8) and (9) are less than $\pm 18.6\%$. The mean value of the absolute value of error is 9.0%. The range of validity of equations (8) and (9) is $2.6 \times 10^3 \leqslant Re \leqslant 2.3 \times 10^4$, $1.53 \leqslant Pr \leqslant 6.43$, and $0.102 \text{ mm} \leqslant D \leqslant 1.09$ mm.

CONCLUSION

An experimental investigation of the heat transfer characteristics of microchannels was performed. Heat transfer coefficients and Nusselt numbers for water flowing through circular channels of diameters 0.76 and 1.09 mm were experimentally determined and found to be higher than would be predicted by traditional Nusselt numbers correlations such as the Gnielinski correlation. The data were compared to data collected by Yu *et al.* [11] and the trends in heat transfer enhancement found to be in agreement. The data suggest that the extent of enhancement (deviation) increases as the channel diameter decreases and Reynolds number increases. Maximum enhancement ratios of nearly 2.5, 1.8 and 1.1 were obtained at Reynolds numbers of $\sim 2 \times 10^4$ for channel diameters of 0.102, 0.76 and 1.09 mm, respectively. A modification of the Gnielinski correlation to accommodate this enhancement caused by the small microchannel diameters was developed from a least squares fit of the experimental data combined with the data of Yu *et al.* With a confidence level of greater than 95%, differences between experimental and predicted Nusselt number values using equations (8) and (9) are less than $\pm 18.6\%$.

Acknowledgements—The authors wish to thank Drs Robert Warrington of Michigan Technological University and Timothy Ameel of the University of Utah for providing the data for the 0.102 mm channel presented in ref. [11]. Discussion with Drs Warrington and Ameel is also appreciated. The keen advice of Mr M. F. Dowling on the setup and calibration of various instruments and the data acquisition system is greatly appreciated.

REFERENCES

1. Kakac, S., Shah, R. and Aung, W., *Handbook of Single-Phase Convective Heat Transfer*. Wiley, New York, 1987.
2. Levy, S., Fuller, R. and Niemi, R., Heat transfer to water in thin rectangular channels. *Journal of Heat Transfer*, 1959, **1**, 129–143.
3. Lancet, R., The effect of surface roughness on the convection heat-transfer coefficient for fully developed turbulent flow in ducts with uniform heat flux. *Journal of Heat Transfer*, 1959, **1**, 168–174.
4. Gambill, W. and Bundy, R., HFIR heat transfer studies of turbulent water flow in thin rectangular channels. ORNL-3079 UC-80-Reactor Technology, Oak Ridge National Laboratory, Oak Ridge, TN, 1961.
5. Acosta, R., Muller, R. and Tobias, C., Transport processes in narrow (capillary) channels. *AIChE Journal*, 1985, **31**, 473–482.
6. Nayak, D., Hwang, L., Turlik, I. and Reisman, A., A high performance thermal module for computer packaging. *Journal of Electronic Materials*, 1987, **16**, 357–364.
7. Hwang, L., Turlik, I. and Reisman, A., Thermal module design for advanced packaging. *Journal of Electronic Materials*, 1987, **16**, 347–355.
8. Phillips, R., Micro-channel heat sinks. In *Advances in Thermal Modeling of Electronic Components*, Vol. 2, ed. A. Bar-Cohen and A. Kraus. ASME Press, New York, 1990, Chapter 3.
9. Wang, B. and Peng, X., Experimental investigation on liquid forced-convection heat transfer through microchannels. *International Journal of Heat and Mass Transfer*, 1994, **37**, 73–82.
10. Peng, X. and Peterson, G., Convective heat transfer and flow friction for water flow in microchannel structures.

International Journal of Heat and Mass Transfer, 1996, **39,** 2599–2608.

11. Yu, D., Warrington, R., Barron, R. and Ameel, T., An experimental investigation of fluid flow and heat transfer in microtubes. *Proceedings of the ASME/JSME Thermal Engineering Conference*, Vol. 1. American Society of Mechanical Engineers, 1995, pp. 523–530.
12. Klein, S. and Alvarado, F., EES—Engineering Equation Solver, F-Chart Software, Middleton, WI, 1992.
13. Petukhov, B., Kurganov, V. and Gladuntsov, A., Heat transfer in turbulent pipe flow of gases with variable properties. *Heat Transfer Soviet Research*, 1973, **5,** 109–116.
14. Gnielinski, V., New equations for heat and mass transfer in turbulent pipe and channel flow. *International Chemical Engineering*, 1976, **16,** 359–368.
15. Filonenko, G., Hydraulic resistance in pipes. *Teploenergetika*, 1954, **1,** 40–44.